**GRAIN-SURFACE TEXTURAL INDICATORS OF VOLATILES IN TERRESTRIAL MARS-REGOLITH ANALOGS: IMPLICATIONS FOR INTERPRETING SAND AND SILT IMAGED BY THE PHOENIX OPTICAL MICROSCOPE AT THE PHOENIX MARS LANDER LANDING SITE.**

M.A. Velbel[1], B.D. Wade[2], I.L. Walker[3], A.E. Veach[3], N. Vanderroest[3], A.N. Niehaus[3], E.N. Lee[3], J.J. Kim[3], A.M. Grant[3], A.M. Fine[3], and J.M. Backlas[3], [1] Michigan State University, Department of Geological Sciences, East Lansing, MI, USA 48824-1115 (velbel@msu.edu), [2]Michigan State University, Department of Plant, Soil & Microbial Sciences, [3]Michigan State University, Honors College.

**Introduction:** The Phoenix Mars Lander landed in Vastitas Borealis, near Mars' northern polar cap, on May 25 2008, and operated until November 2, 2008. The landing site is in a valley dominated by periglacial polygonal patterned ground with 3 to 6 meter polygons, with a thin layer of basaltic sand overlying permafrost [1-7]. Depth to ice was 2-6 cm. A Robotic Arm (RA) dug trenches and acquired samples of dry soil and sublimation residues from water ice. The RA delivered samples to several instrument packages containing a variety of scientific instruments, including an Optical Microscope (OM). The OM imager was equipped with a fixed-focus, fixed-magnification optical system, two lenses, and LEDs in red, blue, green and ultraviolet for simulating color imaging. OM image spatial resolution was determined by the pixel dimension of 4 μm/pixel [8]. A variety of substrates were distributed on a rotating wheel the movement of which enabled the OM to focus and photograph each sample individually [8]. Previous research has classified grain types by color (black and brown) [9], quantified grain form by measuring the long and short dimensions of individual grains directly from OM images [10], and measured particle sizes and size distributions [11].

This presentation describes early results of an investigation to re-interpret grain shapes of the coarsest grains imaged by the Phoenix OM by comparison with grains from the same size fractions of well-studied terrestrial (basaltic) analogs of Mars' surface materials.

**Materials and Methods:** Three terrestrial materials widely regarded by the community as being analogous to fine-grained Mars regolith ("soil") were examined. NASA JSC Mars-1 Mars Soil Simulant consists of glassy phyllosilicate-poor palagonitic volcanic ash from the late Pleistocene Pu'u Nene cinder cone at 1850 m elevation above mean sea level (AMSL) on the south flank of Mauna Kea volcano on Hawai'i [12]. HWMK600 consists of phyllosilicate-poor palagonitic volcanic tephra collected at 3730 m elevation AMSL along the side road to the Very Long Baseline Array (VLBA) Telescope on Mauna Kea [13, 14]. The Mojave Mars Simulant (MMS) consists of granular fractions collected from the Saddleback Basalt near Boron, California, in the Western Mojave Desert [15]. MMS was suggested as a Mars soil simulant because JSC Mars-1 was found to be too hygroscopic, gaining moisture too quickly during experiments to measure water sublimation loss on excavated permafrost under ambient Mars conditions [15]. All three analog materials have been previously documented to contain the primary rock-forming mineral plagioclase [12, 14-16], along with other phases.

Grains from each sample were mounted on aluminum stubs using carbon adhesive tabs, coated with carbon, and imaged using a JEOL 6610LV scanning electron microscope in secondary electron imaging mode (SEM-S) with energy dispersive spectroscopy (EDS). Context images of each entire mount were acquired at the same resolution as the OM (4 μm/pixel), and 150 grains from each sample were imaged at one grain per frame to survey grain-surface textures.

**Results:** *JSC Mars-1*. Vesicles (Fig. 1) ranging in size up to lengths comparable to grain dimensions occur on more than one-third of the grains examined. Fine particulate debris resolvable in whole-frame images of individual grains occurs on about one-tenth of the grains. Networks of intersecting and randomly oriented shallow cracks that appear to be confined to grain surfaces (Fig. 2) occur on more than half of the grains.

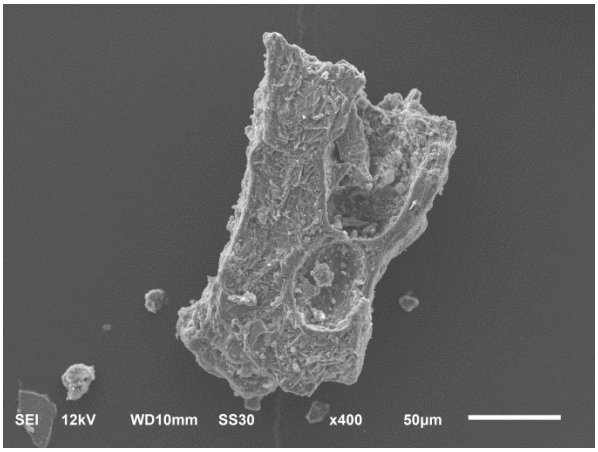


**Figure 1.** Vesicles exposed at the surface of a volcanic ash particle from JSC Mars-1. SEM-S image.

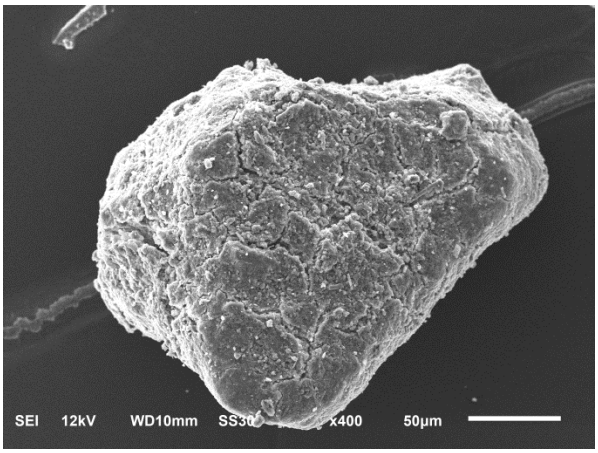


**Figure 2.** Shallow cracks, possibly indicating dehydration, on the surface of a volcanic ash particle from JSC Mars-1. SEM secondary electron image.

*HWMK600*. Vesicles ranging in size up to lengths comparable to grain dimensions occur on approximately one-fourth of the grains. Fine particulate debris resolvable in whole-frame images of individual grains occurs on all grains. Cracks occur on less than one-fifth of the grains. Cracks apparently confined to the surface material on the grain are more abundant than cracks that go deeper into the grain itself.

*MMS*. Over one-third of all grains exhibit at least some planar surfaces approximately perpendicular to one another; this is consistent with the cleavage planes of plagioclase, known from prior work to be present in the basalt from which MMS was prepared [16]. Fine particulate debris resolvable in whole-frame images of individual grains is the dominant grain-surface texture on more than one-half of the grains

**Discussion:** The vesicles in JSC Mars-1 and HWMK600 indicate volcanic eruptions of volatile-bearing magma. Such volatiles contributed to global atmospheric inventories at the time of eruption, but may or may not have been locally abundant in the local environment at the time of tephra alteration. The persistence of primary rock-forming minerals (e.g., plagioclase), and the absence of any instances of common primary-mineral chemical-weathering textures [17-20], in all three analogs examined for this study suggests limited duration and/or intensity of water-driven chemical weathering in the three analog environments.

The difference in the abundance of grains with cracked surfaces between Mauna Kea palagonitic tephras JSC Mars-1 (more than one-half) and HWMK600 (less than one-fifth) may be associated with the climate histories and moisture regimes of the two sample localities. Liquid water likely occurred more frequently and persistently at the lower elevation of the JSC Mars-1 sample site (1850 m AMSL) than at the colder (glaciated and presently periglacial, cold-desert) higher elevation site from which HWMK600 was collected (3730 m). Differences in moisture regimes between the two elevation-controlled temperature regimes may have produced different proportions of extensively weathered grain-surfaces (hydrous and therefore more prone to dehydration cracking), with a higher proportion of hydrous, crack-prone grain surfaces at the lower elevation and "wetter" JSC Mars-1 site and a lower proportion at the higher, cooler, "drier" HWMK600 site.

Vesicles in the two Mauna Kea analog materials (e.g., Fig. 1), indicative of the presence of volatiles in the magma during eruption, are in many instances large enough to have been visible at OM resolution. Common aqueous-corrosion features of the dominant rock-forming minerals at Mars' surface (pyroxene, olivine [17-20]), and the apparent dehydration cracks on grain surfaces from Mars regolith analog materials (Fig. 2), are too small to have been imaged at OM-achievable resolution. Consequently, the significance of the OM imagery for assessing habitability remains under-constrained.

**References:** [1] Arvidson R. E. et al. (2008) *JGR, 113*, E00A03, doi:10.1029/2007JE003021. [2] Mellon M. T. et al. (2008) *JGR, 113*, E00A23, doi:10.1029/2007JE00303. [3] Seelos K. D. et al. (2008) *JGR, 113*, E00A13, doi:10.1029/2008JE003088. [4] Heet T. L. et al. (2009) JGR, 113, E00E04, doi:10.1029/2009JE003416. [5] Mellon M. T. et al. (2009) *JGR, 114*, E00E06, doi:10.1029/2009JE003418. [6] Levy J. S. et al. (2010) *Icarus, 206*, 229-252. [7] Gallagher C. et al. (2011) *Icarus, 201*, 458-471. [8] Hecht M. H. et al. (2008) *JGR, 113*, E00A22, doi:10.1029/2008JE003077. [9] Goetz W. et al. (2010) *JGR, 115*, E00E22. [10] Goetz W. et al. (2010) *LPS XLI*, Abstract #2738. [11] Pike W. T. et al. (2011) *GRL, 38*, L24201. [12] Allen C. C. et al. (1998) *EOS, Transact. AGU, 79*, 129-136. [13] Morris R V. et al. (2000) *JGR, 105*, E1757-E1817. [14] Morris R. V. et al. (2001) *JGR, 106*, E5057-E5083. [15] Peters G. H. (2008) *Icarus, 197*, 470-479. [16] Dibblee T. W. Jr. (1967) *USGS PP* 522 [17] Velbel M. A. (2007) *Developments in Sedimentology 58*, 113-150. [18] Velbel M. A. and Barker W. W. (2008) *Clays & Clay Minerals 56*, 111-126. [19] Velbel M. A. and Losiak A. I. (2010) *J. Sed. Res., 80*, 771-780. [20] Velbel M. A. (2009) *GCA, 73*, 6098-6113.